Three Polyhedron-Based Metal-Organic Frameworks Exhibiting Excellent Acetylene Selective Adsorption

Xia Zhou ,[a†] Zitong Song ,[a†] Rajamani Krishna ,[b‡] Lixiaoxiao Shi ,[a†] Kangli Zhang ,[a†] and Dongmei Wang[*,a†]

[†]Key Laboratory of the Ministry of Education for Advanced Catalysis Materials, College of Chemistry and Materials Sciences, Zhejiang Normal University, Jinhua 321004 P.R. China

[‡]Van 't Hoff Institute for Molecular Sciences University of Amsterdam, Science Park 904, Amsterdam 1090 GE, Nederland

[*]E-mail: dmwang@zjnu.edu.cn

Content

Materials and Synthesize Methods

1.1 Synthesize of JLU-Liu22[1]

A mixture of $Cu(NO_3)_2 \cdot 3H_2O$ (8 mg, 0.033 mmol), H_4tpta (2 mg, 0.005 mmol), N, N-dimethylacetamide (DMA) (1 mL), H_2O (0.65 mL), 0.65 mL of HNO_3 (2.7 M in DMF) was sealed in a glass bottle and then heated in the oven at 85 °C for 24 hours and then 105 °C for 12 h. The mixture was then cooled to room temperature. Bright-blue block crystals were obtained and air-dried (yield 60%, based on H_4tpta).

1.2 Synthesize of JLU-Liu46[2]

A mixture of $Cu(BF_4)_2 \cdot 6H_2O$ (7.5 mg, 0.012 mmol), H_4L (2 mg, 0.005 mmol), 1,4-diazabicyclo[2.2.2]-octane (DABCO) (0.1 mL, 2 g in 10 mL DMF), N,N-dimethylformamide (DMF) (1 mL), ethanol (0.5 mL), H_2O (0.5 mL), and 0.35 mL of HNO_3 (2.7 M in DMF) was sealed in a glass bottle and then heated in the oven at 85 °C for 12 h. Blue crystals were gathered, washed with DMF, and air-dried (58% yield based

on $Cu(BF_4)_2 \cdot 6H_2O$).

1.3 Synthesize of In/Cu-CBDA[3]

The mixture of $In(NO_3)_3 \cdot 4H_2O$ (10 mg, 0.03 mmol), $Cu(NO_3)_3 \cdot 3H_2O$ (8 mg, 0.03 mmol), H_4L (4 mg, 0.01 mmol), N,N-dimethylacetamide (DMA, 0.5 mL), N-methylformamide (NMF, 0.5 mL), deionized water (H_2O, 0.5 mL) and 0.35 mL of HNO_3 (2.7 M in DMA) was sealed in a glass bottle and then heated in the oven at 90 °C for 24 h. After finishing this series of operations, the blue block-shaped crystals of In/Cu-CBDA were collected, washed with fresh DMF, and airdried (yield: 73%, based on CBDA).

Gas Sorption Measurements

Gas sorption and desorption isotherms were measured on an Autosrob iQ. Before adsorption measurements, to remove all the guest solvents in the frameworks. The collected **JLU-Liu22** was washed with DMA several times, and then were first solvent-exchanged with dry ethanol at least three days. **JLU-Liu46** was washed with DMF several times and replaced with absolute ethanol (12 cycles for 3 days). The as-synthesized **In/Cu-CBDA**, washed with fresh DMA, and then were solvent-exchanged with dry acetone at least three days. Then, **JLU-Liu46**, **JLU-Liu22** and **In/Cu-CBDA** were activated under a dynamic vacuum at 373K for 10 h, respectively, which was used for gas adsorption tests.

Adsorption Enthalpy Calculation

The C_2H_2, C_2H_4 and C_2H_6 adsorption enthalpy (Q_{st}) of **JLU-Liu22**, **JLU-Liu46** and **In/Cu-CBDA** were calculated using adsorption data at 273 K and 298 K. A virial-type expression (eqn S1) was used to fit these data, and then the Q_{st} was then calculated by the expression given by eqn S2.

$$\ln P = \ln N + \frac{1}{T}\sum_{i=0}^{m} a_i N^i + \sum_{i=0}^{n} b_i N^i \qquad \text{eqn (S1)}$$

$$Q_{st} = -R\sum_{i=0}^{m} a_i N^i \qquad \text{eqn (S2)}$$

Here, *P*, *N*, and *T* are the pressure (mmHg), amount adsorbed (mmol g $^{-1}$), and temperature (K), respectively. m and n determine the number of terms required to adequately describe the isotherm. a_i and b_i are virial coefficients.

Calculation procedures of selectivity from IAST

The measured experimental data is excess loadings (q^{ex}) of the pure components C_2H_2, C_2H_4 and C_2H_6 for **JLU-Liu22**, **JLU-Liu46**and **In/Cu-CBDA**, which should be converted to absolute loadings (q) firstly.

$$q = q^{ex} + \frac{pV_{pore}}{ZRT} \qquad \text{eqn (S3)}$$

Here *Z* is the compressibility factor. The Peng-Robinson equation was used to estimate the value of compressibility factor to obtain the absolute loading, while the measure pore volume is also necessary.

In order to perform the IAST calculations, the single-component isotherm was fitted by the dual-site Langmuir-Freundlich (DSLF) adsorption model to correlate the pure-component equilibrium data and further predict the adsorption of mixtures. The DSLF model is described as:

$$q = q_{m_1} \times \frac{b_1 \times p^{1/n_1}}{1 + b_1 \times p^{1/n_1}} + q_{m_2} \times \frac{b_2 \times p^{1/n_2}}{1 + b_2 \times p^{1/n_2}} \qquad \text{eqn (S4)}$$

$$S_{ij} = \frac{x_1/x_2}{y_1/y_2} \qquad \text{eqn (S5)}$$

Here p is the pressure of the bulk gas at equilibrium with the adsorbed phase (kPa), q is the adsorbed amount per mass of adsorbent (mol kg^{-1}), q_{m1} and q_{m2} are the saturation capacities of sites 1 and 2 (mol kg^{-1}), b_1 and b_2 are the affinity coefficients of sites 1 and 2 (1/kPa), n_1 and n_2 are the deviations from an ideal homogeneous surface. To investigate the separation of binary mixtures, the adsorption selectivity is defined by x_1 and x_2 are the component loadings of the adsorbed phase in the mixture.

Transient breakthrough simulations

Transient breakthrough simulations were performed for 33.33/33.33/33.33 $C_2H_2/C_2H_4/C_2H_6$, 50/50 C_2H_2/C_2H_4, and 50/50 C_2H_2/C_2H_6 mixtures in **JLU-Liu46**

operating at 100 kPa and 298 K , using the methodology described in earlier publications[4-6] For the breakthrough simulations, the following parameter values were used: length of packed bed, L = 0.3 m; voidage of packed bed, ε = 0.4; volumetric flow rate at the entrance to the bed, Q_0 = 40 L s^{-1}

Grand Canonical Monte Carlo (GCMC) Simulations

Metropolis Monte Carlo method[7] in Sorption module of Materials Studio (MS) 2020 was employed to investigate the sorption behaviors of C_2H_2, C_2H_4 and C_2H_6 molecule upon MOF of **JLU-Liu46**. The interaction analysis included density field distribution and isosteric heat. In present sorption process, the well-known Metropolis algorithm was used to accept or reject a configurational move of considered molecules. The Berendsen thermostat was used for temperature control. 1000000 steps of Metropolis Monte Carlo calculations were carried out with the initial equilibration period of 100000 steps.

S1. Supporting Figurers

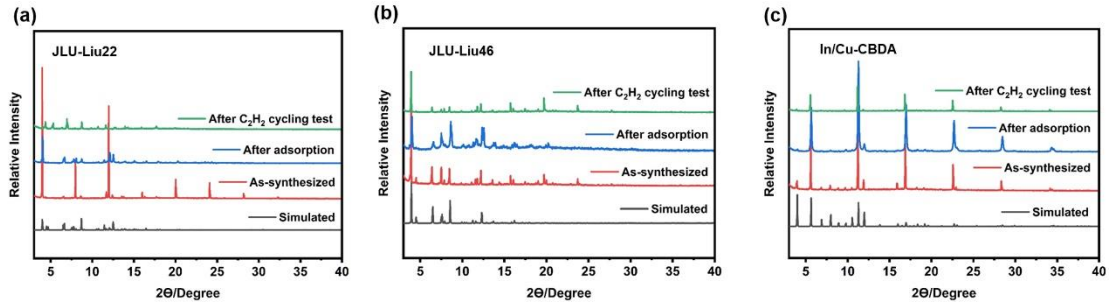

Figure S1. Simulated, as-synthesized, activated-sample and after C_2H_2 cycling test PXRD patterns of (a) **JLU-Liu22**, (b) **JLU-Liu46** and (c) **In/Cu-CBDA**.

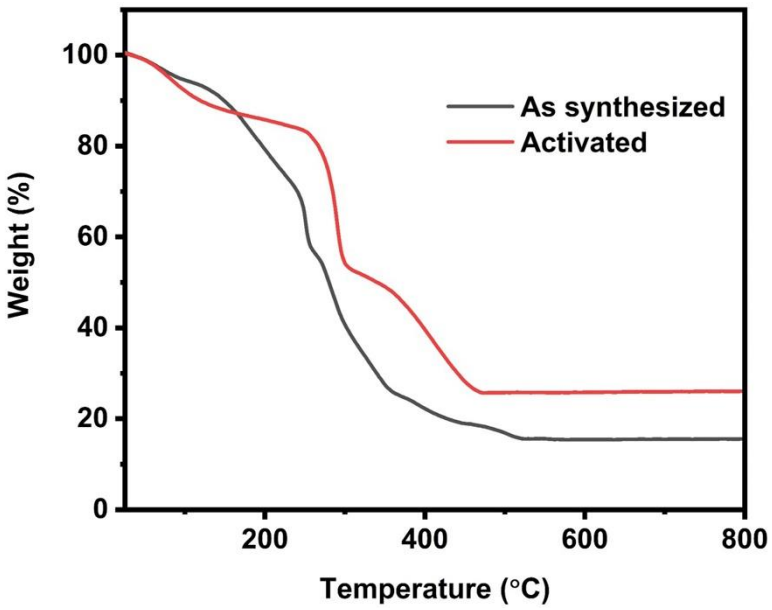

Figure S2. The as-synthesized and activated samples of TGA curves of **JLU-Liu46**.

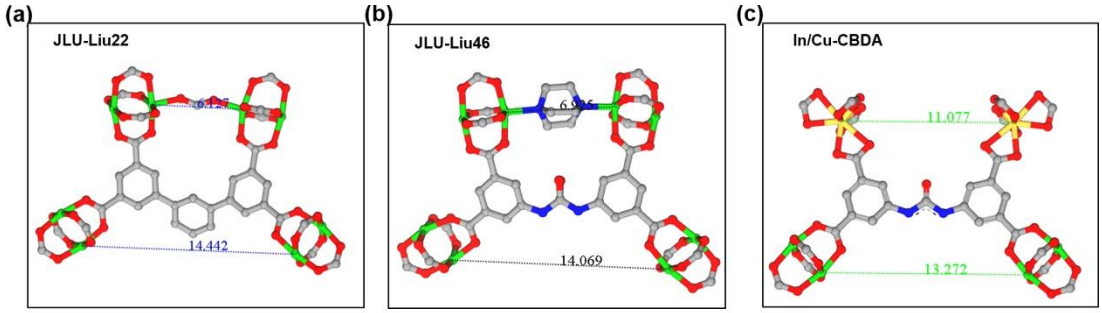

Figure S3. The center distance of the terminal benzenes of (a) **JLU-Liu22**, (b) **JLU-Liu46** and (c) **In/Cu-CBDA**.

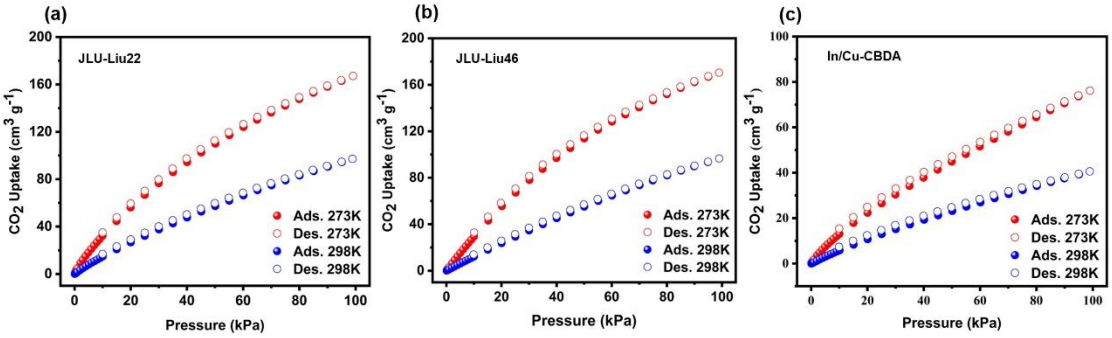

Figure S4. CO_2 adsorption and desorption isotherms of (a) **JLU-Liu46**, (b) **JLU-Liu22** and (c) **In/Cu-CBDA** at different temperatures.

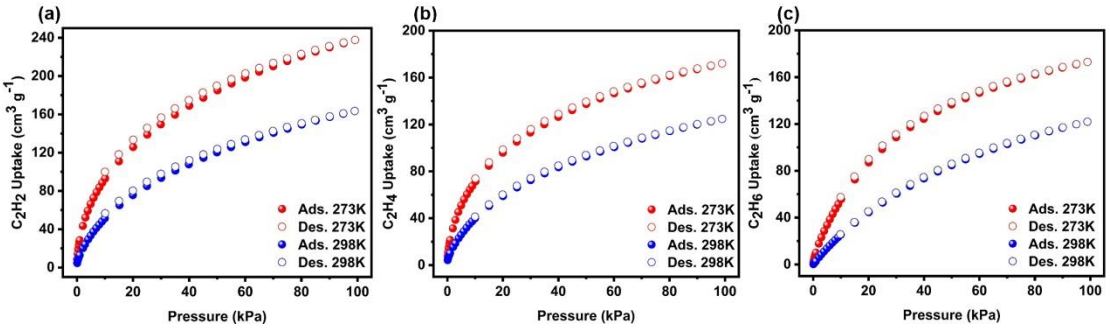

Figure S5. The adsorption and desorption isotherms of (a) C_2H_2, (b) C_2H_4 and (c) C_2H_6 for **JLU-Liu22** at different temperatures.

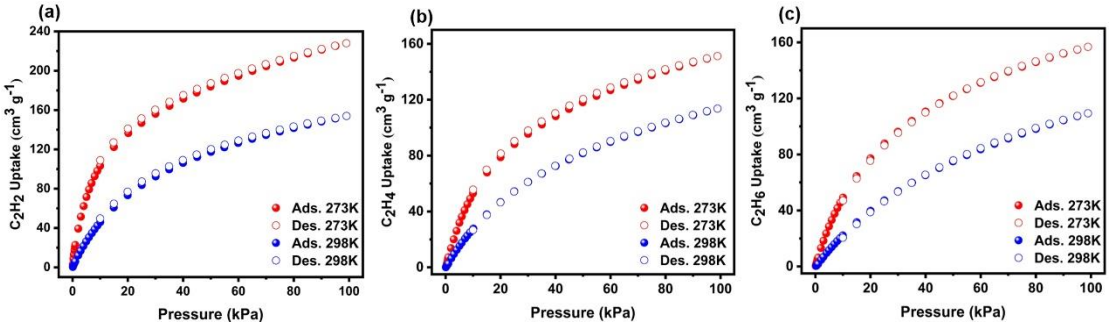

Figure S6. The adsorption and desorption isotherms of (a) C_2H_2, (b) C_2H_4 and (c) C_2H_6 for **JLU-Liu46** at different temperatures.

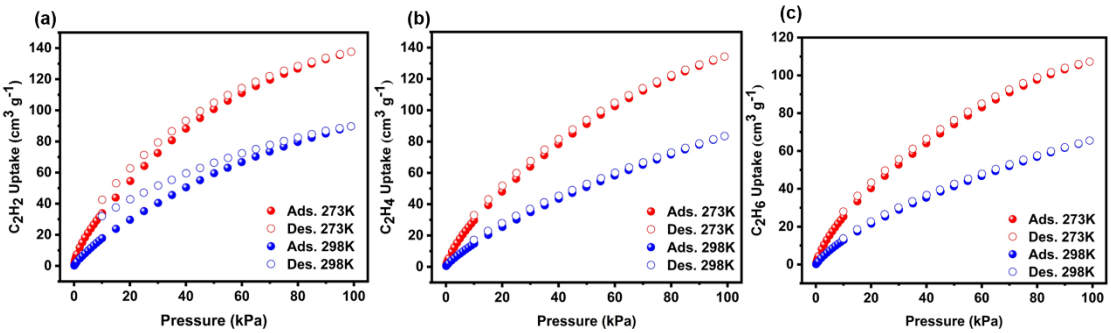

Figure S7. The adsorption and desorption isotherms of (a) C_2H_2, (b) C_2H_4 and (c) C_2H_6 for **In/Cu-CBDA** at different temperatures.

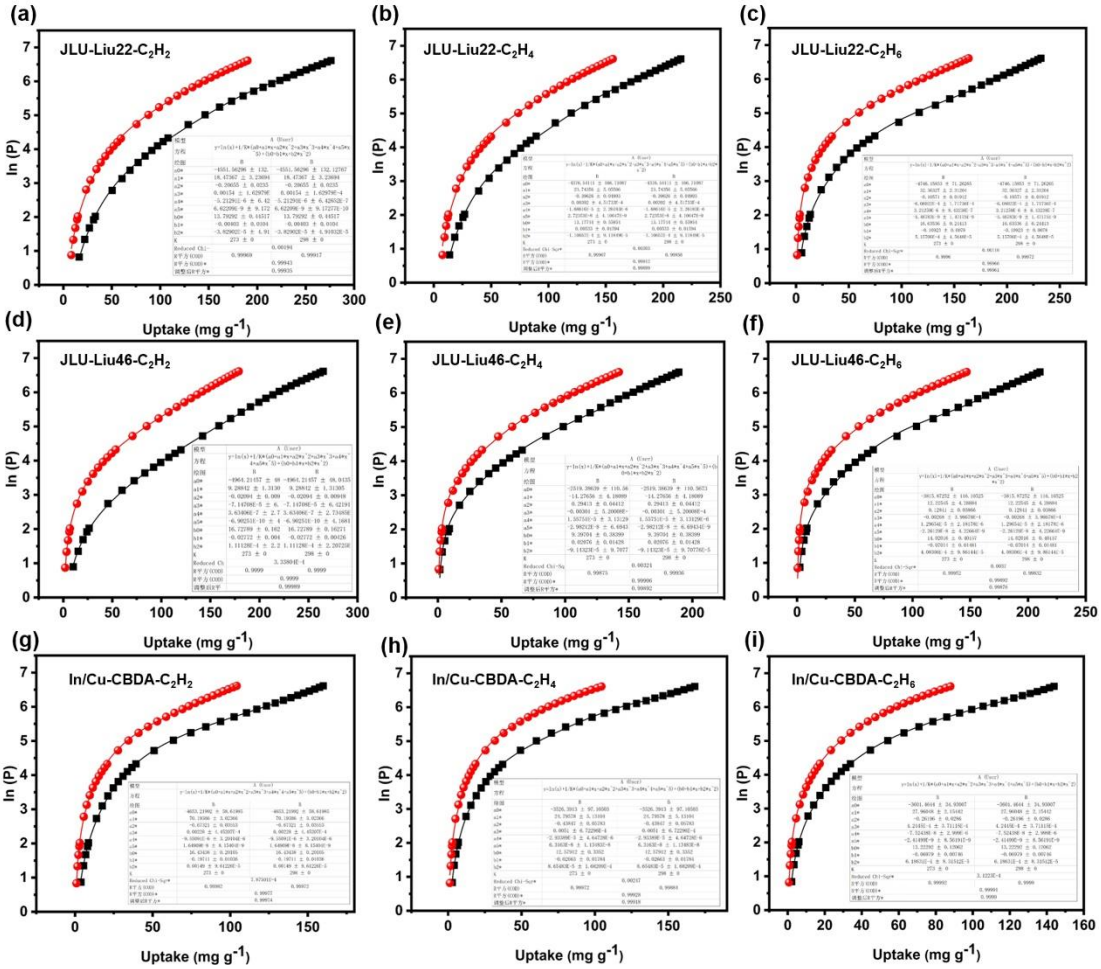

Figure S8. The fitting results of Q_{st} for (a) C_2H_2, (b) C_2H_4 and (c) C_2H_6 in **JLU-Liu22**, (d) C_2H_2, (e) C_2H_4 and (f) C_2H_6 in **JLU-Liu46**, (g) C_2H_2, (h) C_2H_4 and (i) C_2H_6 in **In/Cu-CBDA** by using adsorption isotherms at 298 K.

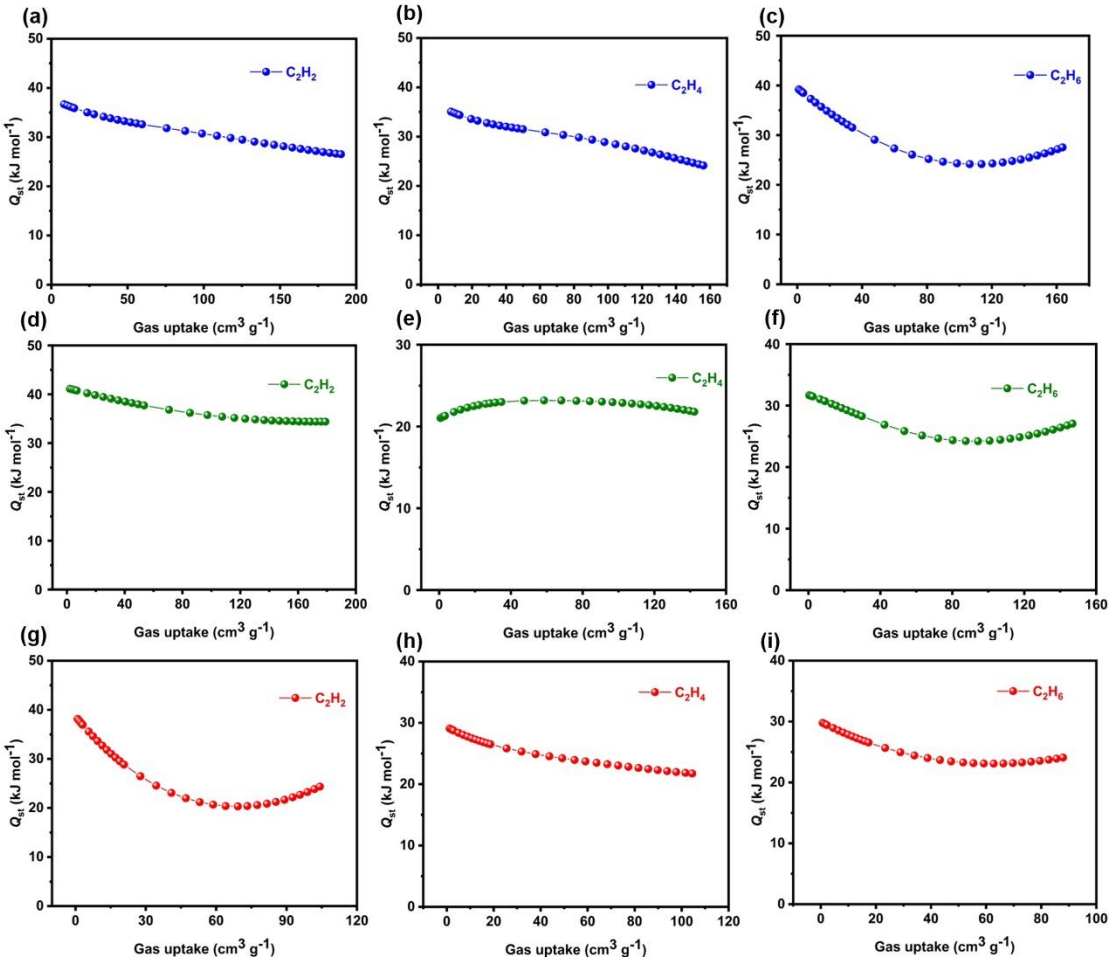

Figure S9. Q_{st} of C_2H_2, C_2H_4 and C_2H_6 for (a-c) **JLU-Liu22**, (d-f) **JLU-Liu46** and (g-i) **In/Cu-CBDA**, respectively.

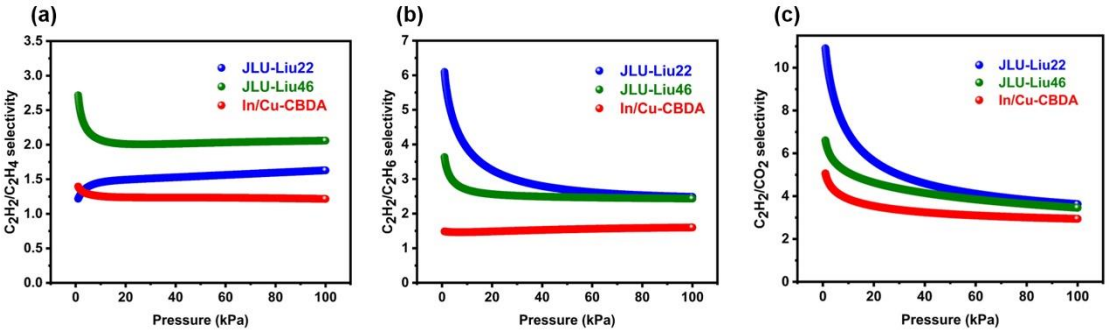

Figure S10. (a) C_2H_2/C_2H_4 (50/50), (b) C_2H_2/C_2H_6 (50/50) and (c) C_2H_2/CO_2 (50/50) adsorption selectivity are predicted by IAST at 298 K and 1 atm for compounds.

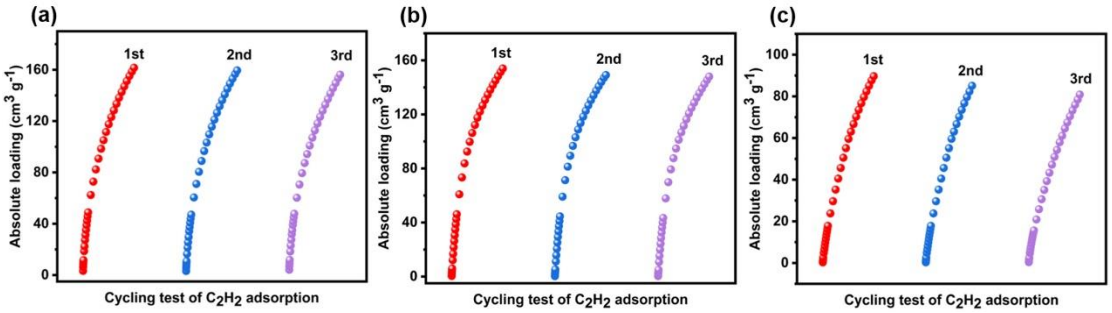

Figure S11. Repetitive C_2H_2 adsorption measurements of (a) **JLU-Liu22**, (b) **JLU-Liu46** and (c) **In/Cu-CBDA** at 298 K.

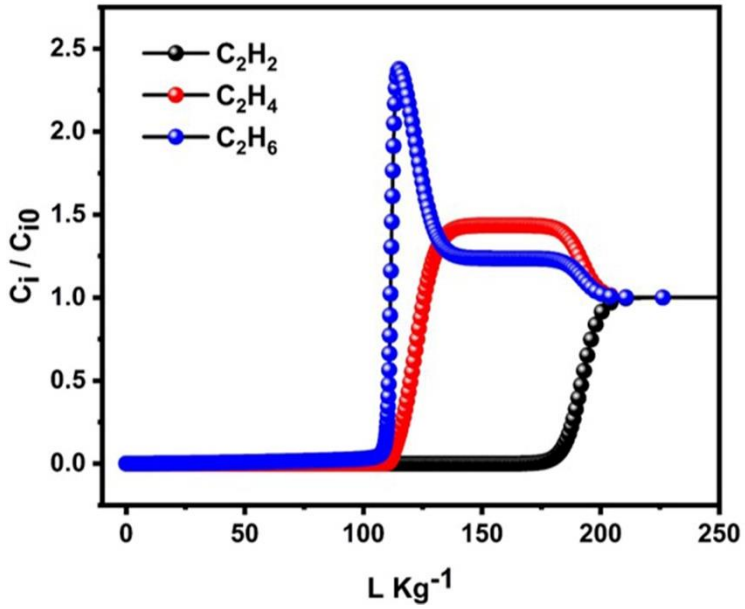

Figure S12. Simulations of transient breakthrough characteristics curves of **JLU-Liu46** for equimolar two-component $C_2H_2/C_2H_4/ C_2H_6$ mixtures at 100 kPa and 298 K

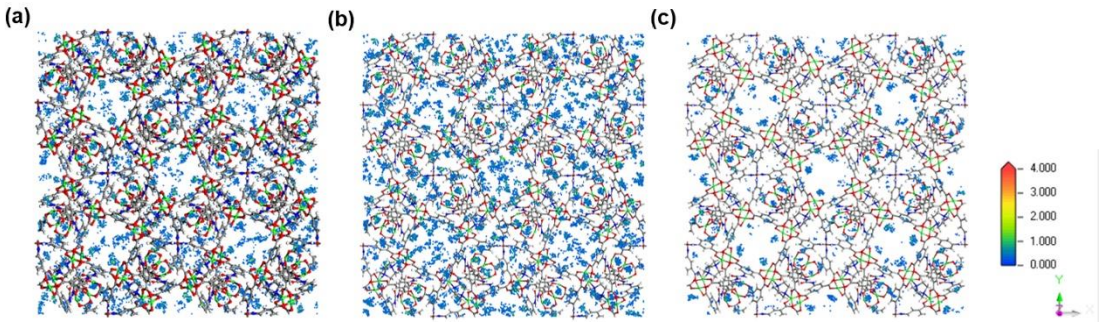

Figure S13. Density distribution of (a) C_2H_2, (b) C_2H_4 and (c) C_2H_6 molecules center-of-mass of **JLU-Liu46** at 298 K and 1 bar simulated by GCMC.

S2. Supporting Tables

Table S1. Physicochemical characteristics of different gasses relevant to their separation.

Molecules	**C_2H_2**	**C_2H_4**	**C_2H_6**
Dimensions (Å^3)	3.32×3.34×5.70	3.28×4.18×4.84	4.08×3.81×4.82
Kinetic diameter (Å)	3.3	4.2	4.4
Quadrupole moment ($\times10^{26}$ esu cm^2)	3.0	1.5	0.65
Polarisability (Å^3)	3.33-3.93	4.25	4.48
Boiling point (K)	189.4	169.5	184.6

Table S2. Summary of gas adsorption data for C_2H_2 separation materials at 298K and 1 bar.

Materials	**C_2H_2 Uptake (cm^3 g^{-1})**	**C_2H_2 Q_{st} (kJ mol^{-1})**	**Ref**
JLULiu-22	163.5	36.67	**This work**
JLULiu-46	153.9	41.11	**This work**
UPC-200(Fe)-F-BIM	139.7	20.5	[8]
PCP-33	121.8	27	[9]
MUF-15	109	24.5	[10]
JNU-2	103	15.8	[11]
NUM-12a	99.1	38.1	[12]
In/Cu-CBDA	89.7	38.2	**This work**
SIFSIX-3-Ni	74	36.7	[13]
UTSA-300a	68.9	57.6	[14]
JNU-1	60	13	[15]
BSF-1	52.6	31	[16]

Table S3. The refined parameters for the Dual-site Langmuir-Freundlich equations fit for the pure isotherms of C_2H_2, C_2H_4, C_2H_6 and CO_2 for **JLU-Liu22** at 298 K.

Adsorbate	**q_{m1} [mmol g^{-1}]**	**b_1 [kPa^{-1}]**	**n_1**	**q_{m2} [mmol g^{-1}]**	**b_2 [kPa^{-1}]**	**n_2**	**R^2**
C_2H_2	10.61993	0.0125	1	1	0.7435	0.9828	0.9996
C_2H_4	0.80603	0.7788	1	7.93224	0.0147	1	0.9996
C_2H_6	0.3035	0.1200	1.2596	9.35462	0.0095	1.0541	1
CO_2	1	0.0587	0.9914	11.6487	0.0015	1.2324	1

Table S4. The refined parameters for the Dual-site Langmuir-Freundlich equations fit for the pure isotherms of C_2H_2, C_2H_4, C_2H_6 and CO_2 for **JLU-Liu46** at 298 K.

Adsorbate	q_{m1} [mmol g^{-1}]	b_1 [kPa^{-1}]	n_1	q_{m2} [mmol g^{-1}]	b_2 [kPa^{-1}]	n_2	R^2
C_2H_2	9.59215	0.0315	0.9141	1	0.0038	1	0.9999
C_2H_4	2.36693	0.0355	1.1303	8.0345	0.006	1	0.9999
C_2H_6	0.95615	0.0277	1.2884	9.34812	0.0075	1	0.9999
CO_2	17.03436	0.00302	1.02426	0.00229	1	1	1

Table S5. The refined parameters for the Dual-site Langmuir-Freundlich equations fit for the pure isotherms of C_2H_2, C_2H_4, C_2H_6 and CO_2 for **In/Cu-CBDA** at 298 K.

Adsorbate	q_{m1} [mmol g^{-1}]	b_1 [kPa^{-1}]	n_1	q_{m2} [mmol g^{-1}]	b_2 [kPa^{-1}]	n_2	R^2
C_2H_2	5.76379	0.0023	1.3518	1	0.1060	0.9461	1
C_2H_4	1	0.0769	1	8.59628	0.0015	1.2603	0.9999
C_2H_6	1	0.0672	0.9520	7.72961	0.0018	1.1606	1
CO_2	0.30548	0.04109	1.13753	10.07197	0.00116	1.09449	1

References

(1) Wang, D.; Liu, B.; Yao, S.; Wang, T.; Li, G.; Huo, Q.; Liu, Y. A Polyhedral Metal-Organic Framework Based on the Supermolecular Building Block Strategy Exhibiting High Performance for Carbon Dioxide Capture and Separation of Light Hydrocarbons. *Chem. Commun.* **2015**, *51* (83), 15287-15289.

(2) Liu, B.; Yao, S.; Liu, X.; Li, X.; Krishna, R.; Li, G.; Huo, Q.; Liu, Y. Two Analogous Polyhedron-Based Mofs with High Density of Lewis Basic Sites and Open Metal Sites: Significant CO_2 Capture and Gas Selectivity Performance. *ACS Appl. Mater. Interfaces* **2017**, *9* (38), 32820-32828.

(3) Wang, D.; Zhang, Y.; Gao, J.; Ge, G.; Li, C. A Polyhedron-Based Heterometallic Mof Constructed by Hsab Theory and Sbb Strategy: Synthesis, Structure, and Adsorption Properties. *Cryst. Growth Des.* **2019**, *19* (8), 4571-4578.

(4) Krishna, R. The Maxwell–Stefan Description of Mixture Diffusion in Nanoporous Crystalline Materials. *Microporous Mesoporous Mater.* **2014**, *185*, 30-50.

(5) Krishna, R. Methodologies for Evaluation of Metal–Organic Frameworks in Separation Applications. *RSC Advances* **2015**, *5* (64), 52269-52295,

(6) Krishna, R. Screening Metal–Organic Frameworks for Mixture Separations in Fixed-Bed Adsorbers Using a Combined Selectivity/Capacity Metric. *RSC Advances* **2017**, *7* (57), 35724-35737.

(7) Metropolis, N.; Rosenbluth, A. W.; Rosenbluth, M. N.; Teller, A. H.; Teller, E. Equation of State Calculations by Fast Computing Machines. *J. Chem. Phys.* **1953**, *21* (6), 1087-1092.

(8) Fan, W.; Yuan, S.; Wang, W.; Feng, L.; Liu, X.; Zhang, X.; Wang, X.; Kang, Z.; Dai, F.; Yuan, D.; Sun, D.; Zhou, H. C. Optimizing Multivariate Metal-Organic Frameworks for Efficient C_2H_2/CO_2 Separation. *J. Am. Chem. Soc.* **2020**, *142* (19), 8728-8737.

(9) Duan, J.; Jin, W.; Krishna, R. Natural Gas Purification Using a Porous Coordination Polymer with Water and Chemical Stability. *Inorg. Chem.* **2015**, *54* (9), 4279-4284.

(10) Qazvini, O. T.; Macreadie, L. K.; Telfer, S. G. Effect of Ligand Functionalization

on the Separation of Small Hydrocarbons and CO_2 by a Series of Muf-15 Analogues. *Chem. Mater.* **2020**, *32* (15), 6744-6752.

(11) Xie, X.-J.; Zeng, H.; Xie, M.; Chen, W.; Hua, G.-F.; Lu, W.; Li, D. A Metal-Organic Framework for C_2H_2/CO_2 Separation under Highly Humid Conditions: Balanced Hydrophilicity/Hydrophobicity. *Chem. Eng. J.* **2022**, *427*, 132033.

(12) Zhang, Q.; Yang, S. Q.; Zhou, L.; Yu, L.; Li, Z. F.; Zhai, Y. J.; Hu, T. L. Pore-Space Partition through an Embedding Metal-Carboxylate Chain-Induced Topology Upgrade Strategy for the Separation of Acetylene/Ethylene. *Inorg. Chem.* **2021**, *60* (24), 19328-19335.

(13) Zhang, Z.; Ding, Q.; Cui, J.; Cui, X.; Xing, H. Fine-Tuning Pore Dimension in Hybrid Ultramicroporous Materials Boosting Simultaneous Trapping of Trace Alkynes from Alkenes. *Small* **2020**, *16* (49), e2005360.

(14) Lin, R. B.; Li, L.; Wu, H.; Arman, H.; Li, B.; Lin, R. G.; Zhou, W.; Chen, B. Optimized Separation of Acetylene from Carbon Dioxide and Ethylene in a Microporous Material. *J. Am. Chem. Soc.* **2017**, *139* (23), 8022-8028.

(15) Zeng, H.; Xie, M.; Huang, Y. L.; Zhao, Y.; Xie, X. J.; Bai, J. P.; Wan, M. Y.; Krishna, R.; Lu, W.; Li, D. Induced Fit of C_2h_2 in a Flexible Mof through Cooperative Action of Open Metal Sites. *Angew. Chem., Int. Ed. Engl.* **2019**, *58* (25), 8515-8519.

(16) Zhang, Y.; Yang, L.; Wang, L.; Duttwyler, S.; Xing, H. A Microporous Metal-Organic Framework Supramolecularly Assembled from a Cu(II) Dodecaborate Cluster Complex for Selective Gas Separation. *Angew. Chem., Int. Ed. Engl.* **2019**, *58* (24), 8145-8150.